JACS
JOURNAL OF THE AMERICAN CHEMICAL SOCIETY
pubs.acs.org/JACS
Article

Charged Water Microdroplets Enable Dissociation of Surrounding Dioxygen

Jian Zhou, Qing Wang, Gongkui Cheng, Wei Shen, Richard N. Zare,* and Xiaoyan Sun*

Cite This: https://doi.org/10.1021/jacs.4c12740
Read Online
ACCESS | Metrics & More | Article Recommendations | Supporting Information

ABSTRACT: The cleavage of dioxygen (O_2) into its atomic constituents typically requires harsh conditions and metal catalysts. We present a remarkable discovery demonstrating that dioxygen can be activated, dissociated, and subsequently transformed into the ozone anion (O_3^-) without any catalyst at the air−water interface in charged microdroplet sprays. Using online mass spectrometry, we directly detected the dioxygen splitting products O_3^- and $H_2O{\cdot}O_3^-$ in microdroplets. The high electric field at the air−water interface, along with microlightning between oppositely charged water microdroplets, induces an electrical discharge responsible for the O−O bond cleavage, leading to the formation of reactive oxygen species (ROS). Isotope labeling experiments further reveal that various ROS, i.e., ·OH, CO_3^-, and HCO_4^-, can be generated through the reaction of dioxygen splitting products with water or CO_2. This study introduces a sustainable pathway for molecular oxygen utilization and offers new insights into ROS generation in microdroplets.

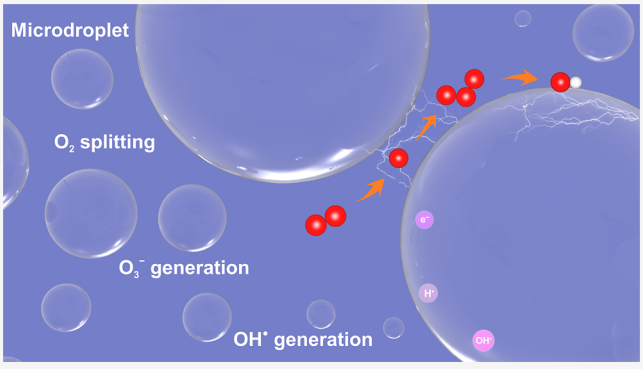

1. INTRODUCTION

Reactive oxygen species (ROS), a collective term of short-lived and highly active oxygen derivatives, include superoxide (O_2^-), ozone (O_3), hydrogen peroxide (H_2O_2), and the hydroxyl radical (·OH).[1−3] These radicals, ions, or molecules play a critical role across various domains, such as cancer treatment,[1] health and disease,[4] plant development,[5] advanced oxidation processes,[6] and catalysis.[7] Traditional methods of ROS generation involve physical, chemical, and biological techniques that often require expensive metal catalysts or enzymes, complicated pretreatment, harsh conditions, and high energy consumption, all of which are not environmentally friendly.[8−11]

In recent years, microdroplet chemistry has emerged as a promising alternative to traditional methods, offering a catalyst-free and green approach to chemical transformations.[12−15] Many distinct characteristics of water microdroplets, including partial solvation,[16,17] ultrahigh electric fields,[18−20] enrichment and alignment of the reagents,[21,22] spontaneous redox reactions,[23,24] and extreme pH conditions,[25,26] play a pivotal role in accelerating reactions and represent a departure from bulk-phase behavior. Recent research has unveiled a range of ROS generated by the strong electric fields at the air−water interface. Hydroxyl radicals can be generated in two ways, one way involves the high electric field (~10^9 V/m) at the surface of microdroplets, which facilitates the extraction of an electron from the hydroxide ion to generate the hydroxyl radical ($OH^- \rightarrow {\cdot}OH + e^-$).[27,28] Another way involves the single electron transfer of surface-bound ions ($OH^- + H^+ \rightarrow {\cdot}OH + {\cdot}H$).[29] Hydrogen peroxide (H_2O_2) can be formed by the recombination of two hydroxyl radicals (·OH + ·OH → H_2O_2) in microdroplets.[15,30] By leveraging these ROS generated by the strong electric fields in water microdroplets, remarkable achievements have been accomplished in organic synthesis, pollutant degradation, and atmospheric chemistry.[13,14]

However, a deep investigation of ROS generated from the surrounding atmosphere, especially the bond scission of dioxygen present in the air surrounding the water droplets, has not been fully explored so far. Superoxide (O_2^-) has been demonstrated to be the reduction product of O_2 by either electron or hydrated electron transfer ($O_2 + e^- \rightarrow O_2^-$).[23,31−33] Nonetheless, detailed investigations of the activation mechanisms have not yet been realized. Oxygen splitting has been suspected in examining lipid oxidation by $H_2{}^{18}O$ isotopic labeling experiments using nanoelectrospray ionization.[34] However, direct evidence of the forms of ROS, and their involvement and mechanisms in microdroplet reactions, remains lacking.

Received: September 13, 2024
Revised: January 18, 2025
Accepted: February 19, 2025

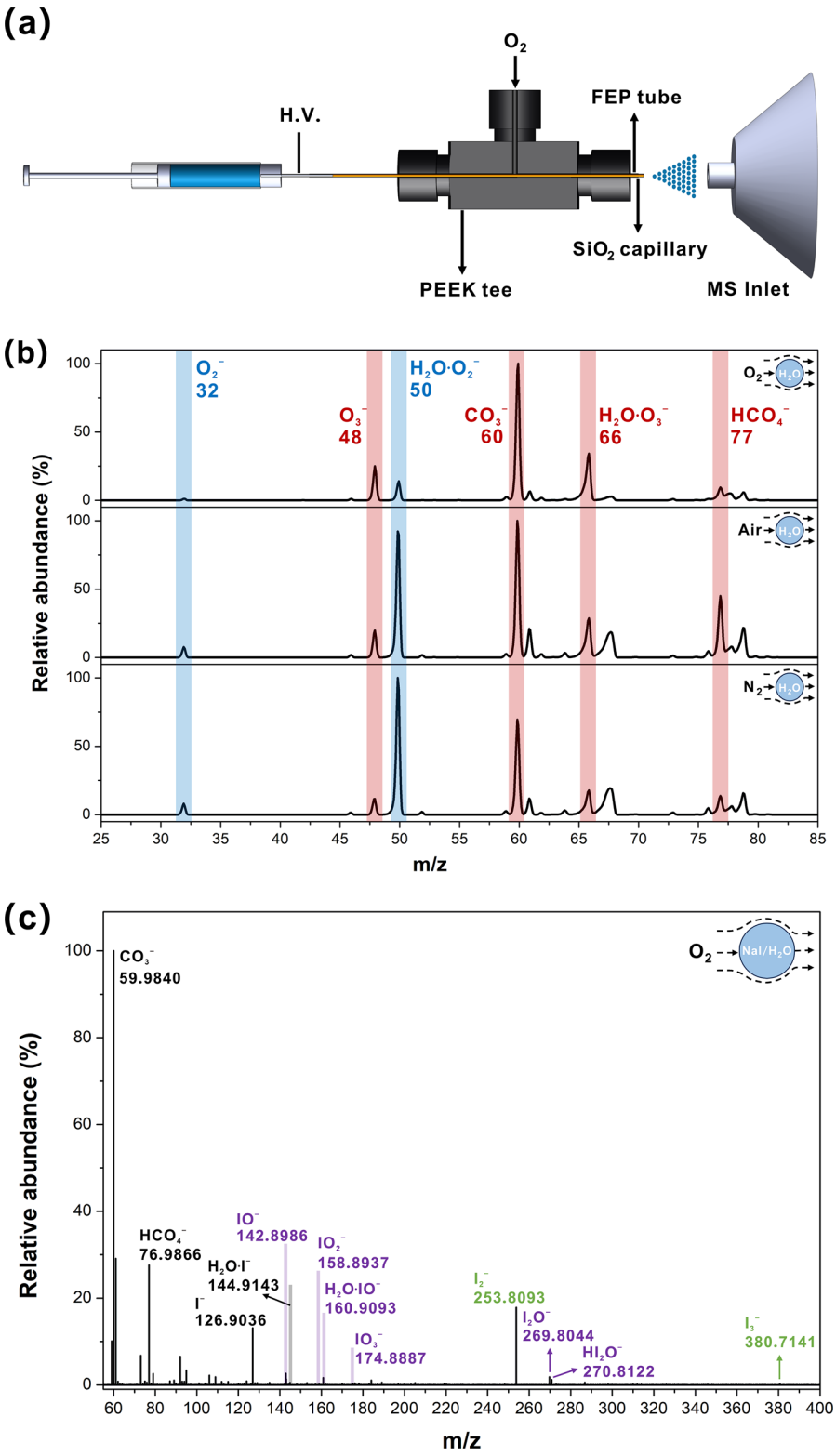

Figure 1. Detecting dioxygen splitting products from aerosolized water. (a) Experimental setup. (b) Mass spectra of sprayed pure water microdroplets with high voltage (−4 kV) and different sheath gases (O_2, compressed air, and N_2), using an ion-trap mass spectrometer for low mass range data acquisition. (c) Mass spectrum of sprayed NaI/H_2O microdroplets with O_2 as the sheath gas under −4 kV, using an Orbitrap mass spectrometer for high-resolution data acquisition. Species marked in blue, red, green, and purple are the products of dioxygen activation, dioxygen splitting, iodide oxidation to ·I, and iodide oxidation to IO_x^-, respectively.

In this study, we present direct evidence of multiple ROS (O_3^-, $H_2O{\cdot}O_3^-$, ·OH, CO_3^-, and HCO_4^-) generated from dioxygen splitting at the air−water interface in charged droplets using online mass spectrometry. The cleavage of the O−O bond in dioxygen, generating those ROS, is attributed to the electrical discharge induced by the high electric field at the air−water interface of charged droplets and microlightning between oppositely charged water microdroplets. Our

https://doi.org/10.1021/jacs.4c12740
J. Am. Chem. Soc. XXXX, XXX, XXX−XXX

investigation underscores the power of water microdroplets for oxygen splitting and complements the well-established ROS generation pathways in microdroplets.

2. RESULTS AND DISCUSSION

The experimental setup is depicted in Figure 1a, with further details provided in the Supporting Information. Pure water (18.2 MΩ·cm) was introduced via a syringe pump through a fused silica capillary positioned inside a larger coaxial capillary. Simultaneously, high-pressure sheath gas (O_2, compressed air, or N_2) was introduced through the outer coaxial capillary. Mass spectra were acquired in negative ion mode under a spray voltage of −4 kV. Reaction kinetics within the water microdroplets were monitored using an ambient mass spectrometer with the microdroplet spray directed toward the instrument.

As shown in Figure 1b, multiple ROS were observed, even with N_2 as the sheath gas. The detection of the superoxide anion (O_2^-, m/z 32) and $H_2O{\cdot}O_2^-$ (m/z 50) at the low mass range suggests that oxygen from the air is activated at the air−water interface of microdroplets, consistent with previous reports.[23,31,33,35] Notably, additional species such as O_3^- (m/z 48), CO_3^- (m/z 60), $H_2O{\cdot}O_3^-$ (m/z 66), and HCO_4^- (m/z 77) were also detected. High-resolution mass spectrometry confirmed the identities of CO_3^- (m/z 59.98526), $H_2O{\cdot}O_3^-$ (m/z 65.99584), and HCO_4^- (m/z 76.98805) with an error of less than 2 ppm relative to their exact mass-to-charge ratios (Figure S1).

Efforts to obtain the collision-induced dissociation (CID) spectrum of $H_2O{\cdot}O_3^-$ (m/z 66) were unsuccessful, as fragmentation of small molecular ions often yields no detectable fragments.[27] However, the CID spectrum of HCO_4^- (m/z 77) revealed the loss of ·OH upon fragmentation (Figure S2). These findings demonstrate that dioxygen in the air is not only activated but also dissociated by the microdroplets, further undergoing transformation into ozone and ozone negative ions, by numerous possible steps[36,37]

$$e^- + O_2 \rightarrow O_2^-$$

$$e^- + O_2 \rightarrow O^- + O$$

$$O^- + O_2 \rightarrow O_3^-$$

$$O + O_2 \rightarrow O_3$$

$$e^- + O_3 \rightarrow O_3^-$$

$$e^- + O_2 \rightarrow O + O + e^-$$

$$O_3 + OH^- \rightarrow HO_2^- + O_2$$

$$HO_2^- + H^+ \rightarrow H_2O_2$$

The inlet capillary temperature of the mass spectrometer was maintained at 30 °C to detect O_3^- (m/z 48) and $H_2O{\cdot}O_3^-$ (m/z 66), as ozone decomposes rapidly at elevated temperatures.[38] The average diameter of microdroplets is around 10 μm (Figure S3) as measured by a laser diffraction particle size analyzer. Further information regarding the reaction distance and O_2 pressure is provided in Figures S4 and S5 in the Supporting Information.

2.1. ROS Quantitation and Identification. To quantify the microdroplets' ability to split dioxygen, we define the oxygen split product percentage (P_{Osplit}) as follows

$$P_{Osplit}/100 = \frac{\Sigma I_{Osplit}}{\Sigma I_{Osplit} + \Sigma I_{Oactivation}} = \frac{I(O_3^-) + I(H_2O{\cdot}O_3^-) + I(CO_3^-) + I(HCO_4^-)}{I(O_3^-)+I(H_2O{\cdot}O_3^-)+I(CO_3^-)+I(HCO_4^-)+I(O_2^-)+I(H_2O{\cdot}O_2^-)}$$

where I denotes the peak intensity of each species. The oxygen splitting product percentage was measured under various sheath gas conditions—pure O_2, compressed air, and N_2—resulting in percentages of 84.5 ± 0.1%, 47.4 ± 1.9%, and 25.1 ± 3.5%, respectively. As the dioxygen concentration increased, the amount of oxygen splitting products also increased, demonstrating the microdroplets' enhanced efficiency in splitting dioxygen under higher oxygen concentrations.

To further investigate the trapping of ROS, 1,2,3-triazole (Tz) was utilized as a trapping agent due to its established ability to capture carbon dioxide in microdroplets.[39,40] When Tz was sprayed with O_2 (Figure S6), a distinct signal for $[Tz-H]^-$ at m/z 68.02533 was detected, along with a novel peak at m/z 101.02307. This peak was identified as $[Tz{\cdot}O_2]^-$ through CID and higher-energy collisional dissociation (HCD) (Figure S7). Additionally, a peak at m/z 117.01802 was assigned to $[Tz{\cdot}O_3]^-$ (Figure S6).

Theoretical calculations confirmed that the trapping of O_2^- and O_3^- by Tz is thermodynamically favorable at the gas−water interface or in the gas phase (Table S4). The successful trapping of O_2^- and O_3^- provides further evidence supporting the activation and splitting of dioxygen.

$H_2{}^{18}O$ isotope labeling experiments were conducted to further determine the origin of the oxygen source of multiple ROS. Compared with the result of pure water (Figure 1b), various ROS composed of ^{16}O were still evident when detecting $H_2{}^{18}O$ (98 atom % of ^{18}O) microdroplets (Figures S8 and 2a). We also used $H_2{}^{18}O$ in lieu of H_2O to prepare the Tz aqueous solution. As shown in Figure S9, no $[Tz{\cdot}{}^{18}O_2]^-$ (m/z 105) and $[Tz{\cdot}{}^{18}O_3]^-$ (m/z 123) were detected, whereas $[Tz{\cdot}O_2]^-$ (m/z 101) and $[Tz{\cdot}O_3]^-$ (m/z 117) remained abundant in the $Tz/H_2{}^{18}O$ sample with O_2 as the sheath gas. This result clearly indicates that the oxygen source of multiple ROS is not derived from the internal water of microdroplets; instead, it originated from the air, as both water and air are the only entities capable of providing a substantial amount of oxygen at the air−water interface of the microdroplet. Collectively, the results of direct ROS capture, ROS trapping, and $H_2{}^{18}O$ isotope labeling demonstrate that dioxygen is activated, split, and further transformed into an ozone anion in microdroplet sprays.

We next provide more evidence for ozone generation in water microdroplet sprays. As demonstrated before, the reaction of ozone and iodide has long been used for ozone detection and removal,[41,42] generating multiple IO_x^- species in addition to ·I, I_2^-, or I_3^-. Figure S10 shows the result of NaI/H_2O microdroplets without the application of high voltage. I_2^- (m/z 253.80929) and I_3^- (m/z 380.71382) were both detected and no IO_x^- species were found, in agreement with a recent report by Zhang and co-workers.[43] They found that in sprayed water microdroplets with N_2, the iodide anion, I^-, can be spontaneously oxidized into ·I, which further evolves into I_2^- and I_3^-, with an interpretation that the formation of ·I may result from the direct removal of an electron from I^- by the high electric field in microdroplets or the oxidation of I^- by ·OH to yield ·I and OH^-. However, under similar conditions except for applying a high voltage (−4 kV), the results were obviously different. In addition to I_2^- and I_3^-, multiple IO_x^-

https://doi.org/10.1021/jacs.4c12740
J. Am. Chem. Soc. XXXX, XXX, XXX−XXX

species such as IO^- (m/z 142.89992), IO_2^- (m/z 158.89486), $H_2O{\cdot}IO^-$ (m/z 160.91053), IO_3^- (m/z 174.88962), I_2O^- (m/z 269.80404), and HI_2O^- (m/z 270.81187) were generated (Figure 1c), consistent with the previous mass spectrometry results of O_3 reacting with iodide.[44] These observations cause us to conclude that I^- was oxidized by the reactive ozone generated in the microdroplet sprays, which in turn provides solid proof that dioxygen must be split and further transformed into ozone by water microdroplets. We also performed the $^{18}O_2$ isotope labeling experiment with spraying of NaI/H_2O microdroplets. As shown in Figure S11, various IO_x^- products with ^{18}O can be detected in the spray of NaI/H_2O microdroplets once $^{18}O_2$ was introduced. This result confirmed that O_3 which further reacts with I^- generating the IO_x^- products is generated from O_2, rather than from ozone contamination in the air.

2.2. Transformation of ROS. Now that dioxygen has been confirmed to be transformed into various ROS in water microdroplet sprays, it is necessary to clarify the transformation and fate of these ROS. It is intriguing to determine how the carbonate radical anion CO_3^- (m/z 60) and HCO_4^- (m/z 77) form in the microdroplets, as shown in Figure 1. Fan et al. recently reported that CO_3^- may be formed by an electron loss of CO_3^{2-} arising from the large electric field at the charged droplet interface during electrospray.[45] However, it is highly probable that the CO_3^- ions observed here are the products of O^- or O_3^- reacting with atmospheric CO_2. To clarify the mechanism, isotope labeling experiments were performed by using $C^{18}O_2$ and $^{18}O_2$, respectively. As shown in Figure 2b, $[C^{18}O_2{\cdot}O]^-$ (m/z 63.99373) species were captured when using O_2 as the sheath gas with a small amount of $C^{18}O_2$ leakage, suggesting that CO_3^- is formed from atmospheric CO_2, rather than residual CO_3^{2-} resulting from dissolving CO_2 in water microdroplets. Figure 2c shows the results of the $^{18}O_2$ isotope labeling experiment by means of O_2 as sheath gas with a small amount of $^{18}O_2$ leakage. In addition to the expected CO_3^- (m/z 59.98526), $[CO_2{\cdot}^{18}O]^-$ (m/z 61.98947) was observed. Interestingly, no obvious $[CO_2{\cdot}^{18}O]^-$ (m/z 61.98947) was detected in $H_2{}^{18}O$ microdroplets (Figure 2a). This finding revealed that the oxygen atom that adds to CO_2 to form CO_3^- (m/z 59.98526) comes from dioxygen, consistent with a previous report using an atmospheric pressure chemical ionization (APCI) source.[46] As a result, we conclude that the carbonate radical anion CO_3^- is the product of highly reactive O^- or O_3^- reacting with atmospheric carbon dioxide ($CO_2 + O^- \rightarrow CO_3^-$; $CO_2 + O_3^- \rightarrow CO_3^- + O_2$).

The peroxymonocarbonate anion (HCO_4^-), the covalent adduct of hydroperoxide anion and carbon dioxide, is proposed to be generated by ·OH reacting with CO_3^- ($\cdot OH + CO_3^- \rightarrow HCO_4^-$) or H_2O_2 reacting with CO_2 ($H_2O_2 + CO_2 \rightarrow H^+ + HCO_4^-$).[47,48] In this case, ·OH and H_2O_2 can be formed in microdroplets or from the split dioxygen reacting with water ($O^- + H_2O \rightarrow \cdot OH + OH^-$; $O_3^- + H_2O \rightarrow \cdot OH + O_2 + OH^-$; $\cdot OH + \cdot OH \rightarrow H_2O_2$). As shown in Figure 2a, the abundance of HCO_4^- (m/z 76.98805) is more significant than that of $[HCO_3{\cdot}^{18}O]^-$ (m/z 78.99223) in $H_2{}^{18}O$ microdroplets. This result suggests that a vast number of hydroxyl radicals are generated from split dioxygen with abundance, outnumbering the spontaneously generated ones. This conclusion is consistent with a previous finding that the presence of O_2 surrounding sprayed water microdroplets increases the concentration of hydrogen peroxide.[15] Apart from the well-established understanding that ·OH is generated by the ultrahigh electric field at the surface of microdroplets that extracts an electron of the hydroxide ion ($OH^- \rightarrow \cdot OH + e^-$) or direct transfer of a single electron from the hydroxide ion ($OH^- + H^+ \rightarrow \cdot OH + \cdot H$),[27−29] there exists another pathway for ·OH generation in charged microdroplets, which is the

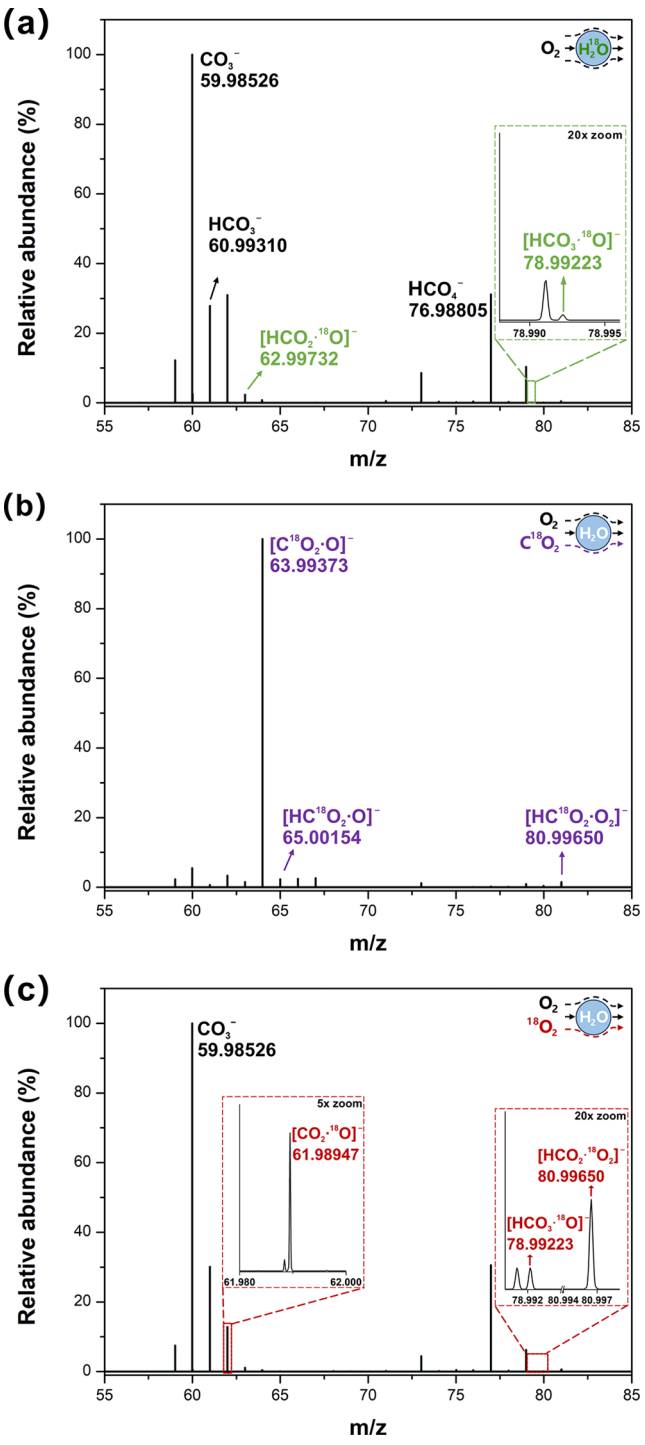

Figure 2. ROS verification through multiple isotope labeling experiments. (a) Mass spectrum of sprayed $H_2{}^{18}O$ (98 atom % of ^{18}O) microdroplets. (b) Mass spectrum of sprayed pure water microdroplets using O_2 as sheath gas with a small amount of $C^{18}O_2$ leakage. (c) Mass spectrum of sprayed pure water microdroplets using O_2 as sheath gas with a small amount of $^{18}O_2$ leakage. Species marked in green, red, and purple are the products resulting from $H_2{}^{18}O$, $C^{18}O_2$, and $^{18}O_2$ labeling, respectively.

https://doi.org/10.1021/jacs.4c12740
J. Am. Chem. Soc. XXXX, XXX, XXX−XXX

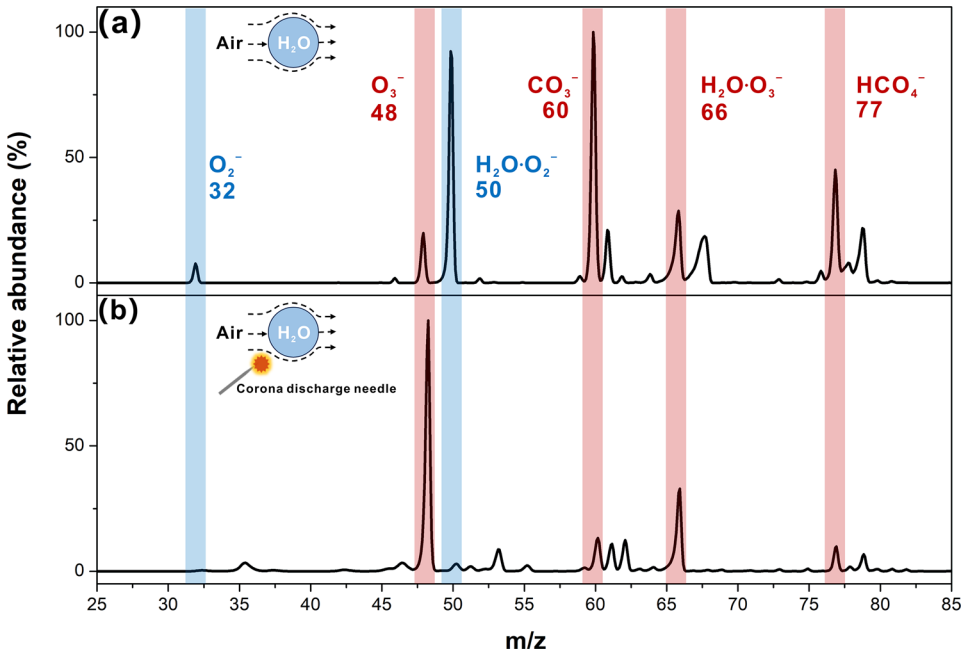

Figure 3. Electrical discharge behavior of water microdroplets. (a) Mass spectrum of sprayed pure water microdroplets with compressed air as sheath gas and high voltage (−4 kV). (b) Mass spectrum of pure water by using a commercial APCI source with compressed air as sheath gas. Species marked in blue and red are the signals of dioxygen activation and splitting products.

dioxygen splitting products reacting with water ($O^- + H_2O \rightarrow \cdot OH + OH^-$; $O_3^- + H_2O \rightarrow \cdot OH + O_2 + OH^-$). As a result, it is crucial to be careful when discussing the origin and impact of hydroxyl radicals in microdroplets.

Hydrogen peroxide (H_2O_2) can be formed by the recombination of two hydroxyl radicals ($\cdot OH + \cdot OH \rightarrow H_2O_2$) from water in microdroplets.[15,30] In this case, many hydroxyl radicals are generated from the surrounding dioxygen ($O^- + H_2O \rightarrow \cdot OH + OH^-$; $O_3^- + H_2O \rightarrow \cdot OH + O_2 + OH^-$), which can further combine together to generate H_2O_2. Meanwhile, during the process of O_2 activation, H_2O_2 may also be generated through the single electron reduction of superoxide ($O_2^- + e^- + 2H^+ \rightarrow H_2O_2$) and two electrons transfer reduction of O_2 generating O_2^{2-} which may further react with water to form H_2O_2 ($O_2 + 2e^- \rightarrow O_2^{2-}$; $O_2^{2-} + 2H_2O \rightarrow H_2O_2 + 2OH^-$).[6,49] Ozone by its reaction with water is also expected to increase the rate of formation of hydrogen peroxide,[37,50] but as shown previously, ozone is not the sole source for producing hydrogen peroxide.[30]

We then reviewed the fate of CO_3^-. As shown in Figure 2a, HCO_3^- (m/z 60.99310) with higher abundance and $[HCO_2 \cdot {}^{18}O]^-$ (m/z 62.99732) were also clearly found in $H_2{}^{18}O$ microdroplets. In addition, in the $C^{18}O_2$ isotope labeling experiment, aside from the detection of $[C^{18}O_2 \cdot O]^-$ (m/z 63.99373), a significant signal of $[HC^{18}O_2 \cdot O]^-$ (m/z 65.00154) was observed as well (Figure 2b). Taken together, these results demonstrate that the bicarbonate HCO_3^- formation is not as straightforward as the common understanding that the dissolved CO_2 forms carbonic acid ($CO_2 + H_2O \rightarrow H_2CO_3$) and then dissociates to produce bicarbonate anions ($H_2CO_3 \rightarrow HCO_3^- + H^+$). In microdroplets, another pathway may predominate. A hydrogen atom transfer (HAT) process may easily occur, where a hydrogen atom split from water induced by the high electric field transfers to a CO_3 radical anion, finally forming the bicarbonate anion ($CO_3^- + H \rightarrow HCO_3^-$). Theoretical calculation results showed that key reactions are thermodynamically favorable in the interfacial region, and detailed calculations can be found in Table S4 of the Supporting Information.

2.3. Mechanisms of Dioxygen Splitting in Microdroplet Sprays. So far, the generation and transformation of the ROS stemming from dioxygen splitting have been clarified by direct capture, ROS trapping, typical iodide oxidation, and isotope labeling. Figuring out the mechanisms of dioxygen splitting is necessary. The high electric field at the air−water interface of microdroplets plays a key role in ROS generation.[13,14] The effect of the spray voltage was investigated, and the result is shown in Figure S12. As the spray voltage drops below −2 kV, the appearance of ROS from the dioxygen is observed. Accordingly, it is speculated that electrical breakdown of dioxygen can occur at the air−water interface of water microdroplets induced by the high electric field. To verify this speculation, experiments of pure water were conducted by using a commercial APCI source with compressed air as sheath gas. As shown in Figure 3b, under the corona discharge condition, all the activated and split oxygen signals found in microdroplets, i.e., O_2^- (m/z 32), O_3^- (m/z 48), $H_2O \cdot O_2^-$ (m/z 50), CO_3^- (m/z 60), $H_2O \cdot O_3^-$ (m/z 66), and HCO_4^- (m/z 77), appeared as well. Additionally, the APCI source was also used for the detection of iodide oxidation products because ozone can be generated under such conditions (Figure S13). Results showed that multiple IO_x^- species found under the corona discharge condition with the APCI source were also observed in the water microdroplets with O_2 as the sheath gas. These results substantiated that electrical breakdown of dioxygen occurs at the air−water interface of charged microdroplets, inducing its splitting. A similar phenomenon has been observed by Banerjee and coworkers; they reported that the high intrinsic electric field at the air−water interface of water microdroplets induces the breakdown of air, resulting in the transformation of nitrogen into its oxides, with detection of N_2^+, NO^+, O_2^+, and NO_2^+.[51]

https://doi.org/10.1021/jacs.4c12740
J. Am. Chem. Soc. XXXX, XXX, XXX−XXX

Scheme 1. Proposed Reaction Mechanisms for O_2 Activation, Splitting, and Transformation into Multiple ROS in Charged Microdroplets[a]

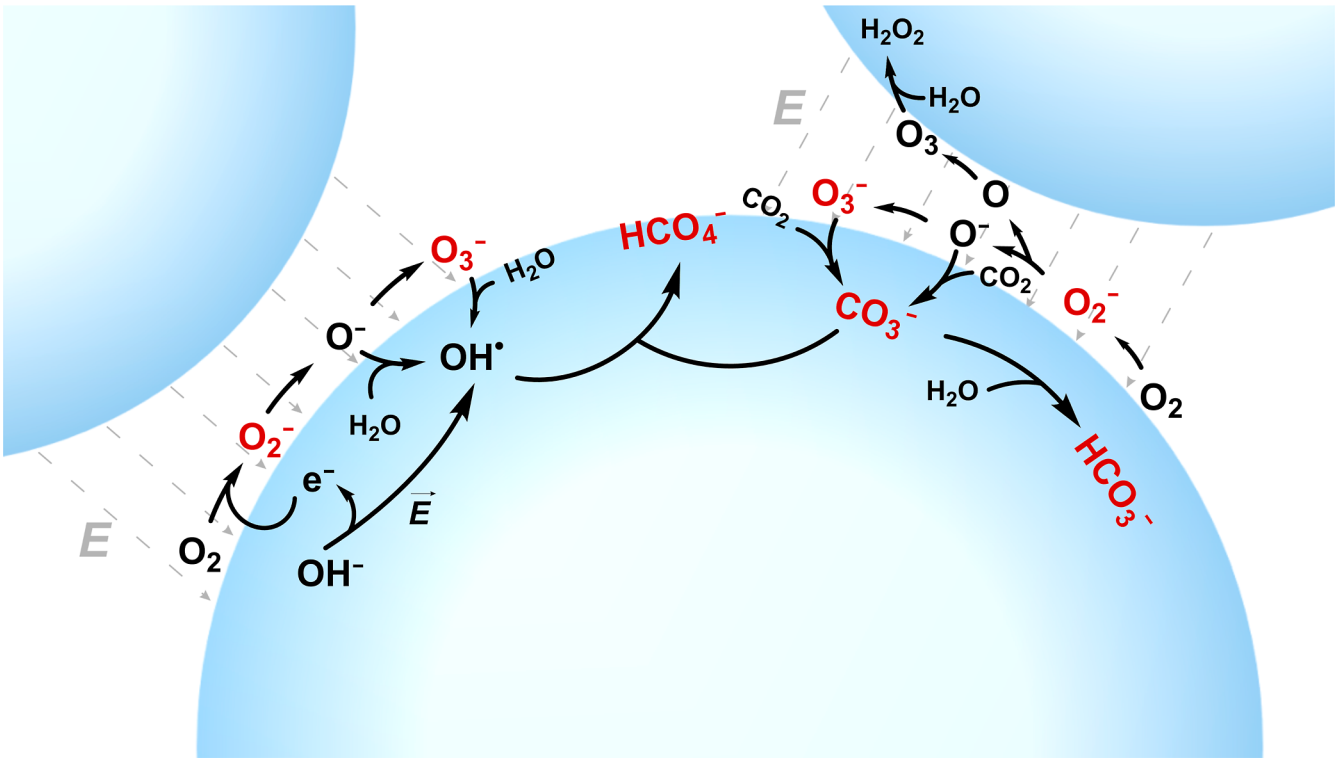

[a]Species marked in red are those observed in the mass spectra

More recently, it was demonstrated that an electrical discharge can occur between oppositely charged microdroplets as they undergo fission in a water spray, generating microlightning that ionizes surrounding neutral gas molecules and breaks molecular bonds.[52] Accordingly, we performed the photon detection experiment to demonstrate microlightning with a photomultiplier tube (PMT) coupled with an oscilloscope parallel to the spray plume. We define the cumulative voltage as the summation of 5000 data points recorded by the oscilloscope during one microsecond. With several tests of light intensity on the response of the PMT, we found that the higher the light intensity, the more negative the voltage value becomes. As shown in Figure S14, a significant reduction of the cumulative voltage occurs when the pure water spray is formed (−70.8 ± 2.5 V, sonic spray) compared with the dark background (−58.5 ± 1.7 V). Moreover, we used a more robust spray voltage (−6.5 kV) to observe microlightning in charged droplets with more fission. As the spray voltage is on, the cumulative voltage further reduced to −77.6 ± 11.5 V. This result indicates that microlightning with photons generation occurs during the droplet splitting process and more photons are generated in this condition as Coulombic fission is more pronounced among the charged droplets, leading to greater droplet separation and generating a greater number of strong electric fields, which will make dioxygen dissociation and ionization more likely. The bond dissociation energy of O_2^- is 360 kJ/mol, which is lower than that of O_2^+ (648 kJ/mol) and O_2 (497 kJ/mol).[53] Consequently, dioxygen splitting is expected to occur more readily in a negatively charged environment. We also conducted the experiment under a positive high voltage (+4 kV), and the resulting dioxygen splitting is significantly less evident than under a negative high voltage, as the level of O_3^+ is nearly undetectable (Figure S15).

We then consider the effect of the solvent. Compared with various ROS detected in water microdroplet sprays, no ROS were detected when utilizing pure methanol or acetonitrile for atomization under the same conditions (Figure S16). Analogous results were obtained using a trapping agent (Tz), where none of the oxygen adduct ions detected in Tz/H_2O were observed when water was replaced with methanol or acetonitrile (Figure S17). These results reveal that the air−water interface of water microdroplets plays a crucial role in the process of dioxygen splitting, where a strong electric field is present. Moreover, a corona discharge, which may occur over the metal emitter during electrospray when the applied voltage exceeds a certain critical value,[54] can be excluded in this case, as we used an insulated silica capillary and a fluorinated ethylene propylene (FEP) tube as components. Furthermore, the experimental results mentioned above can also rule out such a possibility, as no ROS were observed by using methanol or acetonitrile for atomization.

Based on the results above, we propose possible mechanisms for O_2 activation, splitting, and transformation into multiple ROS in microdroplets (Scheme 1). First, dioxygen gains an electron which is pulled out of a hydroxide ion (OH^-) by the strong electric field at the air−water interface or through an electron jump between oppositely charged droplets,[35,52] generating superoxide anion O_2^- ($O_2 + e^- \rightarrow O_2^-$), which in some cases is coordinated to a metal center in oxygen reduction reaction (ORR) electrocatalysis,[55] as observed in the form of O_2^- and $H_2O{\cdot}O_2^-$. Meanwhile, the strong electric field at the air−water interface and microlightning induce the electrical breakdown of dioxygen to be split into O^- ($O_2 + e^-$

https://doi.org/10.1021/jacs.4c12740
J. Am. Chem. Soc. XXXX, XXX, XXX−XXX

$\rightarrow O^- + O$), which can react with O_2 and CO_2, generating O_3^- and CO_3^- ($O^- + O_2 \rightarrow O_3^-$; $O^- + CO_2 \rightarrow CO_3^-$), as observed in the form of O_3^-, CO_3^-, and $H_2O{\cdot}O_3^-$. The generated ozone anion can react with CO_2 to form CO_3^- as well ($CO_2 + O_3^- \rightarrow CO_3^- + O_2$). The hydroxyl radical can be formed through O^- or O_3^- reacting with water ($O^- + H_2O \rightarrow {\cdot}OH + OH^-$; $O_3^- + H_2O \rightarrow {\cdot}OH + O_2 + OH^-$). At the same time, HCO_4^- is generated through CO_3^- reacting with a hydroxyl radical (${\cdot}OH + CO_3^- \rightarrow HCO_4^-$). Then, hydrogen atom transfer (HAT) may easily occur, where one hydrogen atom split from water induced by the high electric field transfers to CO_3^- forming finally the bicarbonate anion ($CO_3^- + H \rightarrow HCO_3^-$).

3. CONCLUSIONS

To recap, we report dioxygen activation, splitting, and transformation into an ozone anion at the air−water interface of charged microdroplets. We provided mass spectrometric observations of various ROS. Dioxygen activation products O_2^- and $H_2O{\cdot}O_2^-$ and dioxygen split products O_3^-, CO_3^-, $H_2O{\cdot}O_3^-$, and HCO_4^- were verified by direct capture, ROS trapping, typical iodide oxidation, isotope labeling, and APCI experiments. It is proposed that dioxygen activation and splitting occur predominantly from an electrical discharge induced by the high electric field at the air−water interface in a microdroplet and microlightning between oppositely charged water microdroplets. The ROS generated from dioxygen can produce a hydroxyl radical by interacting with water. We hope that this study deepens our understanding of the intriguing properties of water microdroplets and helps uncover the hidden channels of ROS generation in microdroplets, which would be inspiring for the potential applications of this technology in environmental science, especially in the in situ treatment of pollutants or in healthcare for sterilization processes.

■ ASSOCIATED CONTENT

Supporting Information

The Supporting Information is available free of charge at https://pubs.acs.org/doi/10.1021/jacs.4c12740.

Detailed experimental and calculation methods, additional experimental and theoretical results (PDF)

■ AUTHOR INFORMATION

Corresponding Authors

Richard N. Zare − *Department of Chemistry, Stanford University, Stanford, California 94305, United States;* orcid.org/0000-0001-5266-4253; Email: zare@stanford.edu

Xiaoyan Sun − *State Key Laboratory of Photoelectric Conversion and Utilization of Solar Energy, Qingdao New Energy Shandong Laboratory, Qingdao Institute of Bioenergy and Bioprocess Technology, Chinese Academy of Sciences, Qingdao 266101, China; University of Chinese Academy of Sciences, Beijing 100049, China;* orcid.org/0000-0003-0035-8371; Email: sunxy@qibebt.ac.cn

Authors

Jian Zhou − *State Key Laboratory of Photoelectric Conversion and Utilization of Solar Energy, Qingdao New Energy Shandong Laboratory, Qingdao Institute of Bioenergy and Bioprocess Technology, Chinese Academy of Sciences, Qingdao 266101, China; University of Chinese Academy of Sciences, Beijing 100049, China*

Qing Wang − *State Key Laboratory of Photoelectric Conversion and Utilization of Solar Energy, Qingdao New Energy Shandong Laboratory, Qingdao Institute of Bioenergy and Bioprocess Technology, Chinese Academy of Sciences, Qingdao 266101, China; University of Chinese Academy of Sciences, Beijing 100049, China*

Gongkui Cheng − *State Key Laboratory of Photoelectric Conversion and Utilization of Solar Energy, Qingdao New Energy Shandong Laboratory, Qingdao Institute of Bioenergy and Bioprocess Technology, Chinese Academy of Sciences, Qingdao 266101, China*

Wei Shen − *State Key Laboratory of Photoelectric Conversion and Utilization of Solar Energy, Qingdao New Energy Shandong Laboratory, Qingdao Institute of Bioenergy and Bioprocess Technology, Chinese Academy of Sciences, Qingdao 266101, China*

Complete contact information is available at: https://pubs.acs.org/10.1021/jacs.4c12740

Notes

The authors declare no competing financial interest.

■ ACKNOWLEDGMENTS

X.S. acknowledges the financial support of QIBEBT (Grant: QIBEBT S202306), Natural Science Foundation of Shandong Province (ZR2021QB128, ZR2022MA040), and Shandong Province Taishan Young Scholars Project (tsqn201909161). R.N.Z. acknowledges support from Stanford University. We thank Prof. Dr. Xinxing Zhang from Nankai University for helpful suggestions. The numerical calculations in this paper have been done at Hefei's advanced computing center.

■ REFERENCES

(1) Liou, G.-Y.; Storz, P. Reactive Oxygen Species in Cancer. *Free Radic. Res.* **2010**, *44* (5), 479−496.

(2) Bayr, H. Reactive Oxygen Species. *Crit. Care Med.* **2005**, *33* (12), S498−S501.

(3) Huang, L.; Li, Z.; Zhang, X. Radiotracers for Nuclear Imaging of Reactive Oxygen Species: Advances Made So Far. *Bioconjugate Chem.* **2022**, *33* (5), 749−766.

(4) Alfadda, A. A.; Sallam, R. M. Reactive Oxygen Species in Health and Disease. *BioMed. Res. Int.* **2012**, *2012* (1), 1−14.

(5) Mhamdi, A.; Van Breusegem, F. Reactive Oxygen Species in Plant Development. *Development* **2018**, *145* (15), dev164376.

(6) Zhou, L.; Liu, Y.; Shi, H.; Qing, Y.; Chen, C.; Shen, L.; Zhou, M.; Li, B.; Lin, H. Molecular Oxygen Activation: Innovative Techniques for Environmental Remediation. *Water Res.* **2024**, *250*, 121075.

(7) Nosaka, Y.; Nosaka, A. Y. Generation and Detection of Reactive Oxygen Species in Photocatalysis. *Chem. Rev.* **2017**, *117* (17), 11302−11336.

(8) Kim, W.; Tachikawa, T.; Moon, G.; Majima, T.; Choi, W. Molecular-Level Understanding of the Photocatalytic Activity Difference between Anatase and Rutile Nanoparticles. *Angew. Chem., Int. Ed.* **2014**, *53* (51), 14036.

(9) Wan, Z.; Mao, Q.; Chen, Q. Proton-Dependent Photocatalytic Dehalogenation Activities Caused by Oxygen Vacancies of In2O3. *Chem. Eng. J.* **2021**, *403*, 126389.

(10) Bae, Y. S.; Oh, H.; Rhee, S. G.; Yoo, Y. D. Regulation of Reactive Oxygen Species Generation in Cell Signaling. *Mol. Cells* **2011**, *32* (6), 491−509.

(11) Murphy, M. P. How Mitochondria Produce Reactive Oxygen Species. *Biochem. J.* **2009**, *417* (1), 1−13.

(12) Spoorthi, B. K.; Debnath, K.; Basuri, P.; Nagar, A.; Waghmare, U. V.; Pradeep, T. Spontaneous Weathering of Natural Minerals in Charged Water Microdroplets Forms Nanomaterials. *Science* **2024**, *384* (6699), 1012−1017.
(13) Qiu, L.; Cooks, R. G. Spontaneous Oxidation in Aqueous Microdroplets: Water Radical Cation as Primary Oxidizing Agent. *Angew. Chem., Int. Ed.* **2024**, *63* (17), No. e202400118.
(14) Jin, S.; Chen, H.; Yuan, X.; Xing, D.; Wang, R.; Zhao, L.; Zhang, D.; Gong, C.; Zhu, C.; Gao, X.; Chen, Y.; Zhang, X. The Spontaneous Electron-Mediated Redox Processes on Sprayed Water Microdroplets. *JACS Au* **2023**, *3* (6), 1563−1571.
(15) Mehrgardi, M. A.; Mofidfar, M.; Zare, R. N. Sprayed Water Microdroplets Are Able to Generate Hydrogen Peroxide Spontaneously. *J. Am. Chem. Soc.* **2022**, *144* (17), 7606−7609.
(16) Vaitheeswaran, S.; Thirumalai, D. Hydrophobic and Ionic Interactions in Nanosized Water Droplets. *J. Am. Chem. Soc.* **2006**, *128* (41), 13490−13496.
(17) Yan, X.; Bain, R. M.; Cooks, R. G. Organic Reactions in Microdroplets: Reaction Acceleration Revealed by Mass Spectrometry. *Angew. Chem., Int. Ed.* **2016**, *55* (42), 12960−12972.
(18) Meng, Y.; Gnanamani, E.; Zare, R. N. Direct C(Sp3)−N Bond Formation between Toluene and Amine in Water Microdroplets. *J. Am. Chem. Soc.* **2022**, *144* (43), 19709−19713.
(19) Meng, Y.; Gnanamani, E.; Zare, R. N. One-Step Formation of Pharmaceuticals Having a Phenylacetic Acid Core Using Water Microdroplets. *J. Am. Chem. Soc.* **2023**, *145* (14), 7724−7728.
(20) Zhang, D.; Yuan, X.; Gong, C.; Zhang, X. High Electric Field on Water Microdroplets Catalyzes Spontaneous and Ultrafast Oxidative C−H/N−H Cross-Coupling. *J. Am. Chem. Soc.* **2022**, *144* (35), 16184−16190.
(21) Nam, I.; Nam, H. G.; Zare, R. N. Abiotic Synthesis of Purine and Pyrimidine Ribonucleosides in Aqueous Microdroplets. *Proc. Natl. Acad. Sci. U.S.A.* **2018**, *115* (1), 36−40.
(22) Nam, I.; Lee, J. K.; Nam, H. G.; Zare, R. N. Abiotic Production of Sugar Phosphates and Uridine Ribonucleoside in Aqueous Microdroplets. *Proc. Natl. Acad. Sci. U.S.A.* **2017**, *114* (47), 12396−12400.
(23) Qiu, L.; Cooks, R. G. Simultaneous and Spontaneous Oxidation and Reduction in Microdroplets by the Water Radical Cation/Anion Pair. *Angew. Chem., Int. Ed.* **2022**, *61* (41), No. e202210765.
(24) Gong, C.; Li, D.; Li, X.; Zhang, D.; Xing, D.; Zhao, L.; Yuan, X.; Zhang, X. Spontaneous Reduction-Induced Degradation of Viologen Compounds in Water Microdroplets and Its Inhibition by Host−Guest Complexation. *J. Am. Chem. Soc.* **2022**, *144* (8), 3510−3516.
(25) Wang, T.; Li, Z.; Gao, H.; Hu, J.; Chen, H.-Y.; Xu, J.-J. Ultrafast C−C and C−N Bond Formation Reactions in Water Microdroplets Facilitated by the Spontaneous Generation of Carbocations. *Chem. Sci.* **2023**, *14* (41), 11515−11520.
(26) Banerjee, S.; Zare, R. N. Syntheses of Isoquinoline and Substituted Quinolines in Charged Microdroplets. *Angew. Chem. Int. Ed.* **2015**, *54* (49), 14795.
(27) Xing, D.; Meng, Y.; Yuan, X.; Jin, S.; Song, X.; Zare, R. N.; Zhang, X. Capture of Hydroxyl Radicals by Hydronium Cations in Water Microdroplets. *Angew. Chem., Int. Ed.* **2022**, *61* (33), No. e202207587.
(28) Lee, J. K.; Walker, K. L.; Han, H. S.; Kang, J.; Prinz, F. B.; Waymouth, R. M.; Nam, H. G.; Zare, R. N. Spontaneous Generation of Hydrogen Peroxide from Aqueous Microdroplets. *Proc. Natl. Acad. Sci. U.S.A.* **2019**, *116* (39), 19294−19298.
(29) Colussi, A. J. Mechanism of Hydrogen Peroxide Formation on Sprayed Water Microdroplets. *J. Am. Chem. Soc.* **2023**, *145* (30), 16315−16317.
(30) Mofidfar, M.; Mehrgardi, M. A.; Xia, Y.; Zare, R. N. Dependence on Relative Humidity in the Formation of Reactive Oxygen Species in Water Droplets. *Proc. Natl. Acad. Sci. U.S.A.* **2024**, *121* (12), No. e2315940121.
(31) Wang, S.; Yang, J.; Liu, F.; Xiao, S.; Xiao, F.; Dong, X.; Shan, S. Water Microdroplets: A Catalyst-Free Source of Reactive Oxygen Species for Pollutants Removal. *J. Clean. Prod.* **2023**, *420*, 138444.
(32) Song, X.; Basheer, C.; Zare, R. N. Water Microdroplets-Initiated Methane Oxidation. *J. Am. Chem. Soc.* **2023**, *145* (50), 27198−27204.
(33) Li, J.; Xia, Y.; Song, X.; Chen, B.; Zare, R. N. Continuous Ammonia Synthesis from Water and Nitrogen via Contact Electrification. *Proc. Natl. Acad. Sci. U.S.A.* **2024**, *121* (4), No. e2318408121.
(34) Han, Z.; Omata, N.; Matsuda, T.; Hishida, S.; Takiguchi, S.; Komori, R.; Suzuki, R.; Chen, L. C. Tuning Oxidative Modification by a Strong Electric Field Using NanoESI of Highly Conductive Solutions near the Minimum Flow Rate. *Chem. Sci.* **2023**, *14* (17), 4506−4515.
(35) Yuan, X.; Zhang, D.; Liang, C.; Zhang, X. Spontaneous Reduction of Transition Metal Ions by One Electron in Water Microdroplets and the Atmospheric Implications. *J. Am. Chem. Soc.* **2023**, *145* (5), 2800−2805.
(36) Yanallah, K.; Pontiga, F.; Fernandez-Rueda, A.; Castellanos, A.; Belasri, A. Ozone Generation by Negative Corona Discharge: The Effect of Joule Heating. *J. Phys. D: Appl. Phys.* **2008**, *41*, 195206.
(37) Heikes, B. G. Aqueous H_2O_2 Production from O_3 in Glass Impingers. *Atmos. Environ.* **1984**, *18* (7), 1433−1445.
(38) Ershov, B. G.; Morozov, P. A. The Kinetics of Ozone Decomposition in Water, the Influence of PH and Temperature. *Russ. J. Phys. Chem. A* **2009**, *83* (8), 1295−1299.
(39) Song, X.; Meng, Y.; Zare, R. N. Spraying Water Microdroplets Containing 1,2,3-Triazole Converts Carbon Dioxide into Formic Acid. *J. Am. Chem. Soc.* **2022**, *144* (37), 16744−16748.
(40) Gong, K.; Meng, Y.; Zare, R. N.; Xie, J. Molecular Mechanism for Converting Carbon Dioxide Surrounding Water Microdroplets Containing 1,2,3-Triazole to Formic Acid. *J. Am. Chem. Soc.* **2024**, *146* (12), 8576−8584.
(41) Petruci, J. F. d. S.; Barreto, D. N.; Dias, M. A.; Felix, E. P.; Cardoso, A. A. Analytical Methods Applied for Ozone Gas Detection: A Review. *TrAC Trends Anal. Chem.* **2022**, *149*, 116552.
(42) Uchiyama, S.; Inaba, Y.; Kunugita, N. Ozone Removal in the Collection of Carbonyl Compounds in Air. *J. Chromatogr. A* **2012**, *1229*, 293−297.
(43) Xing, D.; Yuan, X.; Liang, C.; Jin, T.; Zhang, S.; Zhang, X. Spontaneous Oxidation of I− in Water Microdroplets and Its Atmospheric Implications. *Chem. Commun.* **2022**, *58* (89), 12447−12450.
(44) Pillar-Little, E. A.; Guzman, M. I.; Rodriguez, J. M. Conversion of Iodide to Hypoiodous Acid and Iodine in Aqueous Microdroplets Exposed to Ozone. *Environ. Sci. Technol.* **2013**, *47* (19), 10971−10979.
(45) Dong, J.; Chen, J.; Wang, W.; Wei, Z.; Tian, Z.-Q.; Fan, F. R. Charged Microdroplets as Microelectrochemical Cells for CO2 Reduction and C−C Coupling. *J. Am. Chem. Soc.* **2024**, *146* (3), 2227−2236.
(46) Ewing, R. G.; Waltman, M. J. Production and Utilization of CO3− Produced by a Corona Discharge in Air for Atmospheric Pressure Chemical Ionization. *Int. J. Mass Spectrom.* **2010**, *296* (1), 53−58.
(47) Salvitti, C.; Pepi, F.; Troiani, A.; Rosi, M.; de Petris, G. The Peroxymonocarbonate Anion HCO4− as an Effective Oxidant in the Gas Phase: A Mass Spectrometric and Theoretical Study on the Reaction with SO2. *Molecules* **2023**, *28* (1), 132.
(48) Bakhmutova-Albert, E. V.; Yao, H.; Denevan, D. E.; Richardson, D. E. Kinetics and Mechanism of Peroxymonocarbonate Formation. *Inorg. Chem.* **2010**, *49* (24), 11287−11296.
(49) Eatoo, M. A.; Mishra, H. Busting the Myth of Spontaneous Formation of H2O2 at the Air−Water Interface: Contributions of the Liquid−Solid Interface and Dissolved Oxygen Exposed. *Chem. Sci.* **2024**, *15* (9), 3093−3103.
(50) Gallo, A.; Musskopf, N. H.; Liu, X.; Yang, Z.; Petry, J.; Zhang, P.; Thoroddsen, S.; Im, H.; Mishra, H. On the formation of hydrogen peroxide in water microdroplets. *Chem. Sci.* **2022**, *13* (9), 2574−2583.
(51) Kumar, A.; Avadhani, V. S.; Nandy, A.; Mondal, S.; Pathak, B.; Pavuluri, V. K. N.; Avulapati, M. M.; Banerjee, S. Water Microdroplets

https://doi.org/10.1021/jacs.4c12740
J. Am. Chem. Soc. XXXX, XXX, XXX−XXX

in Air: A Hitherto Unnoticed Natural Source of Nitrogen Oxides. *Anal. Chem.* **2024**, *96* (26), 10515−10523.
(52) (a) Xia, Y.; Xu, J.; Li, J.; Chen, B.; Dai, Y.; Zare, R. N. Visualization of the Charging of Water Droplets Sprayed into Air. *J. Phys. Chem. A* **2024**, *128* (28), 5684−5690. (b) Meng, Y.; Xia, Y.; Xu, J.; Zare, R. N. Spraying of water microdroplets forms luminescence and causes chemical reactions in surrounding gas. *Sci Adv.* **2025**, *11*, eadt8979.
(53) Luo, Y.-R.. *Comprehensive Handbook of Chemical Bond Energies*, 1st, ed.; CRC Press, 2007.
(54) Hassan, I.; Pavlov, J.; Errabelli, R.; Attygalle, A. B. Oxidative Ionization Under Certain Negative-Ion Mass Spectrometric Conditions. *J. Am. Soc. Mass Spectrom.* **2017**, *28* (2), 270−277.
(55) Pegis, M. L.; Wise, C. F.; Martin, D. J.; Mayer, J. M. Oxygen Reduction by Homogeneous Molecular Catalysts and Electrocatalysts. *Chem. Rev.* **2018**, *118* (5), 2340−2391.

https://doi.org/10.1021/jacs.4c12740
J. Am. Chem. Soc. XXXX, XXX, XXX−XXX